J Biol Inorg Chem (2011) 16:195–208
DOI 10.1007/s00775-010-0716-0

ORIGINAL PAPER

Identification of a potent activator of Akt phosphorylation from a novel series of phenolic, picolinic, pyridino, and hydroxamic zinc(II) complexes

Savvas N. Georgiades · Lok Hang Mak · Inmaculada Angurell · Evelyn Rosivatz · M. Firouz Mohd Mustapa · Christoulla Polychroni · Rudiger Woscholski · Ramon Vilar

Received: 7 July 2010 / Accepted: 7 October 2010 / Published online: 23 October 2010
© SBIC 2010

Abstract The discovery of small-molecule modulators of signaling pathways is currently a particularly active area of research. We aimed at developing unprecedented metal-based activators of Akt signaling which can potentially find applications as tools for regulating glucose metabolism downstream of Akt or serve as lead structures for developing antidiabetic drugs. In this context, a highly diverse library of 11 new zinc(II) complexes with phenolic, picolinic, pyridino, and hydroxamic ligands, all containing features beneficial for medicinal purposes, was prepared and screened in an assay that detected levels of phospho-Akt in lysates from NIH3T3 cells after treatment with the compounds. The complexes featuring hydroxamic ligands were found to be the most prominent activators of Akt among the molecules prepared, with the most efficient compound acting at submicromolar concentrations. Further characterization revealed that this compound induces phosphorylation of the Akt downstream effector glycogen synthase kinase 3β, but does not act as an inhibitor of tyrosine phosphatases or PTEN.

Keywords Zinc · Hydroxamic acid · Phosphorylation · Akt · Phosphoinositide 3-kinase

S. N. Georgiades · I. Angurell · M. Firouz Mohd Mustapa · C. Polychroni · R. Vilar (✉)
Department of Chemistry,
Imperial College London,
Exhibition Road,
London SW7 2AZ, UK
e-mail: r.vilar@imperial.ac.uk

L. H. Mak · E. Rosivatz · R. Woscholski
Division of Cell and Molecular Biology,
Imperial College London,
Exhibition Road,
London SW7 2AZ, UK

Introduction

Small molecules with the ability to modulate cellular signaling have the potential to act as spatial and temporal perturbagens of biological processes, and thus constitute a reversible, practical, easily tuned, and readily accessible alternative to genetic mutations in our study of biological systems [1, 2]. Using chemical tools to interfere with processes that involve protein phosphorylation, for example, has a high likelihood of leading to significant biological consequences (both structural and functional) [3], since it is now well established that in all living systems phosphorylation serves as a universal signal that marks the activation or deactivation of enzymes and signaling cascades [4–8].

A particularly appealing target for modulation is the serine/threonine kinase Akt. The activation of Akt (Fig. 1) is due to the phosphorylation of two sites (Thr-308 and Ser-473) by protein kinases that are controlled by phosphoinositide 3-kinase (PI3K) [9]. PI3K is activated by upstream signals such as insulin binding to its receptor. Numerous reports have linked Akt phosphorylation to critical biological events such as cell growth, proliferation, and survival [10], thus rendering it medicinally significant for cancer [11] and neurological diseases [12] among others. Akt activation has also been implicated in cellular glucose uptake and utilization; consequently, Akt is also a highly relevant target in the development of antidiabetic drugs [13–15].

Identification of new small molecules that make it possible to regulate at will the phosphorylation levels of Akt might yield control over some of these downstream processes. With a focus on the diabetes implications of Akt activation, we have previously shown that a series of vanadium(IV) and vanadium(V) complexes with picolinic

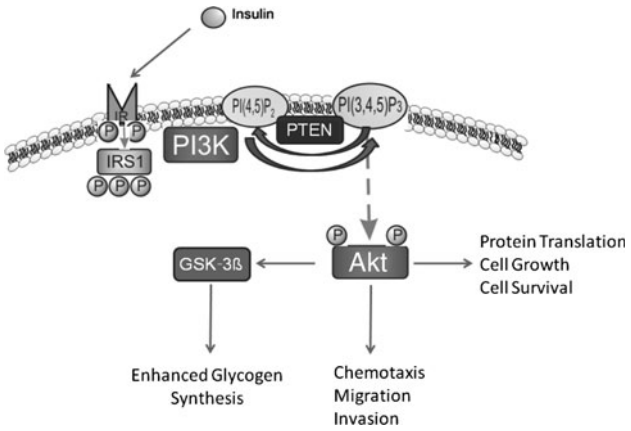

Fig. 1 Simplified representation of the biochemical pathways that connect the insulin receptor (*IR*), phosphoinositide 3-kinase (*PI3K*), and PTEN with Akt and its downstream effector glycogen synthase kinase 3β (*GSK-3β*). *PI(4,5)P_2* phosphatidylinositol 4,5-bisphosphate, *PI(3,4,5)P_3* phosphatidylinositol 3,4,5-trisphosphate

ligands were able to induce Akt phosphorylation, acting by inhibiting PTEN phosphatase, an enzyme upstream of Akt that directly counteracts the function of PI3K [13]. In parallel, other laboratories have suggested that protein tyrosine phosphatases (PTP) are possible targets for complexes of vanadium [16–20]. Recent studies by Sakurai et al. describing metal-based small molecules with the ability to enhance Akt phosphorylation levels have involved zinc(II) as the metal center [21, 22]. Most of these reports have suggested that zinc(II) complexes carry out their effects in a PI3K-dependent mode [23, 24], and that relatively high concentrations of complexes are needed to achieve significant Akt phosphorylation enhancements.

Encouraged by the findings described above and given the relatively limited number of zinc(II) compound classes evaluated as Akt activators so far, we investigated a broader range of zinc(II) compound families, with the aim of identifying novel and more potent small molecules that can find applications as chemical perturbagens of Akt signaling and glucose metabolism. Zinc(II) favorably exhibits low toxicity (especially in comparison with vanadium) as well as the ability to afford complexes with a variety of coordination geometries, spanning from tetracoordination to hexacoordination. These properties were taken into account in the design of our compounds, along with the inclusion of new phenolic, picolinic, pyridino, and hydroxamic ligands, which we considered likely to contribute favorable properties in terms of functional and structural diversity, hydrogen-bonding ability, aqueous solubility, membrane transport, and pharmacokinetics. The synthesis of 11 new zinc(II) complexes (Fig. 2) and their biological evaluation leading to identification of a potent Akt activator is described herein.

Results and discussion

Synthesis of ligands and complexes

As part of our effort to discover new and effective metal-based activators of Akt signaling, we prepared an extended series of zinc(II) complexes, which would be inclusive of a diverse set of ligands. The compound design had to meet certain requirements: the complexes should exhibit distinct coordination geometries and 3D shapes; they should exhibit various patterns of hydrogen-bond donors and acceptors; they should include pharmaceutically beneficial functionalities; they should have good aqueous solubility and membrane permeability; and they should be readily synthesized. We chose to investigate four major classes of ligands, namely phenolic, picolinic (similar to the ones we previously evaluated with vanadium), pyridino, and hydroxamic. The functional groups present in these ligands were deemed compatible with all of the above-mentioned criteria, on the basis of their performance in a multitude of previous pharmaceutical applications. Eleven complexes were synthesized in total, all of which are novel compounds.

The first group of complexes (compounds **1**–**4**, Scheme 1) includes polydentate Schiff base ligands (or their reduced counterparts) derived from salicyl precursors, and these complexes were formed using $Zn(OAc)_2$ as the metal source. Compounds **1** and **2** exhibit an O–N–O coordination pattern in their tridentate ligand. Compound **1** was obtained by condensation of glycine at the 2-aldehyde position of 2,4-di(formyl)phenol in the presence of the metal, followed by a second condensation of the remaining aldehyde moiety to an ethanolamine unit and reduction. Complex **2** was obtained in one step by reacting an α-amino acid, homocysteic acid, with a similar salicyl aldehyde that features a sulfonic acid substituent at the 4-position. The polar functionalities chosen in these compounds confer the desired hydrophilicity and hydrogen-bonding ability to the complexes, both beneficial for the aqueous solubility of the compounds and their potential to interact with biomolecules. As suggested by our study and in agreement with a reported crystal structure of **1a** [25], complexes **1** and **2** were isolated in a hydrated state and in aqueous solution can potentially reach hexacoordination through further hydration. The fact that zinc(II) has no specific preference for a fixed geometry allows water to occupy free coordination sites, which is likely the case for other complexes in this study as well. Ligands for the synthesis of **3** and **4** were prepared from the same aromatic precursor as for **2**. In the case of **3** (which has a ligand-to-metal stoichiometry of 2:1) the organic precursor was modified via reductive amination with *n*-propylamine to afford the N–O bidentate amine ligand **3a** prior to complexation. The ligand in **4** (which exhibits an

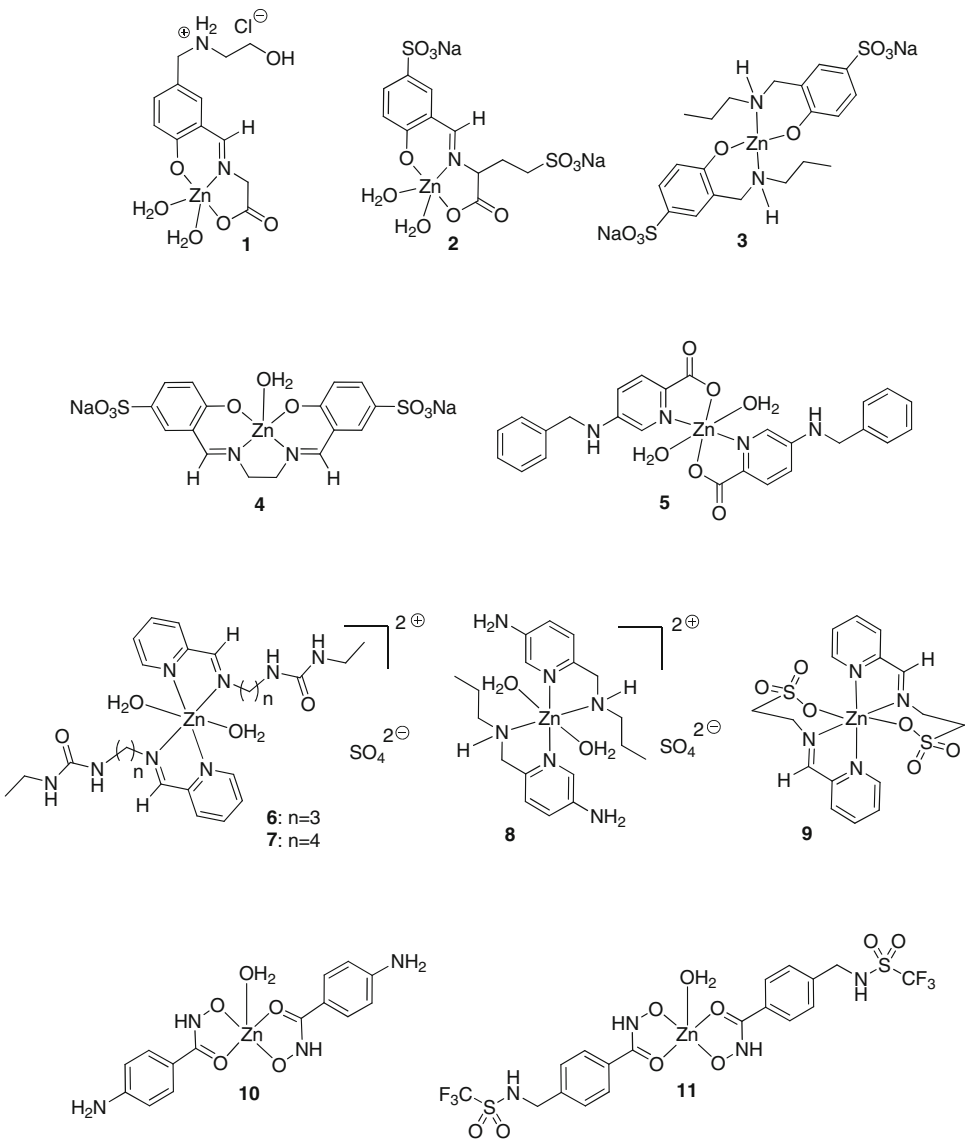

Fig. 2 Proposed structures of all zinc(II) coordination compounds prepared in this study

O–N–N–O coordination pattern) links two precursor molecules via double imine formation upon their condensation with ethylenediamine. The complex likely has distorted pyramidal geometry, as has been demonstrated previously for other zinc(II)–salen complexes [26].

Another bidentate N–O ligand was derived from 5-aminopicolinic acid (Scheme 2). Although this specific complex has not been previously reported, it should be noted that zinc(II) complexes with other derivatives of picolinic acid have been studied previously as insulin mimetics [27–29]. The amine handle was initially modified to afford benzylamine **5a** [30] to explore the impact of this bulky moiety on the biological activity of the corresponding zinc(II) complex. Complex **5** was prepared by reacting the ligand with zinc sulfate under basic conditions.

A group of four ligands were derived from 2-formylpyridines (Scheme 3) via imine formation. In the case of compounds **6b** and **7b** (ligands for **6** and **7**, respectively), the amine components reacting with 2-formylpyridine contained an ethyl urea moiety. In the synthesis of **8**, propylamine was reacted with 5-nitro-2-formylpyridine, and the nitro/imine intermediate **8a** was reduced to the amine/amine ligand **8b**. Complexation to obtain complexes **6–8** was achieved with $ZnSO_4$. In the case of **9**, the zwitterionic amine taurine was reacted with 2-formylpyridine under basic conditions, followed by complexation with $ZnCl_2$ in the same pot. Although this subset of molecules also offers extensive hydrogen-bonding patterns, they have larger steric requirements compared with some of the asymmetric members of the series.

Hydroxamic complexes **10** and **11** were generated as shown in Scheme 4. A benzoic acid functionalized at the 4-position with an amine handle (either directly attached to the ring or as an aminomethyl moiety, respectively) was

Scheme 1 Synthesis of phenolic zinc(II) complexes **1**–**4** (yields **1** 99%, **2** 54%, **3** 70%, **4** 95%). *r.t.* room temperature

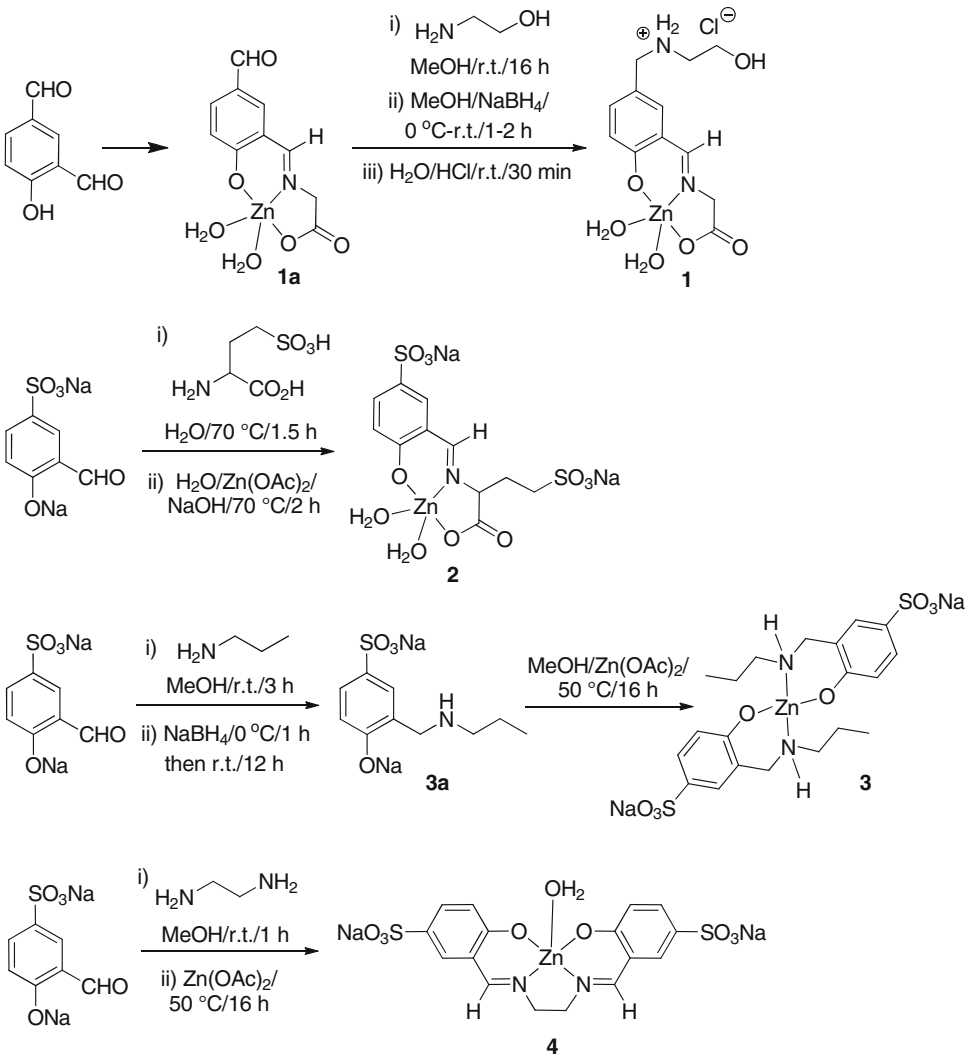

Scheme 2 Synthesis of picolinic zinc(II) complex **5** (yield 34%). *DMF* dimethylformamide

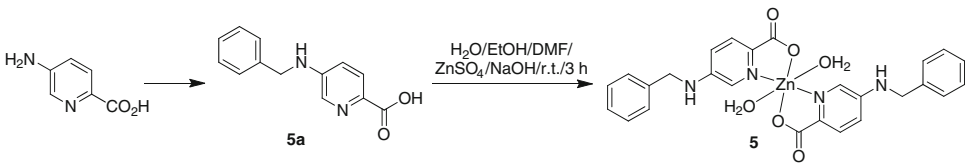

converted to its corresponding methyl ester using known procedures [31, 32]. A critical step in ligand preparation was the transformation of these esters to hydroxamic acids using hydroxylamine sulfate under basic aqueous conditions. Conversion of methyl ester **10a** to hydroxamic acid **10b** was performed in one step [33] leaving the free amine intact, whereas **11a** underwent modification with trifluoromethane sulfonic anhydride to form sulfonamide **11b**, prior to its conversion to the desired hydroxamic acid **11c**. Ligands **10b** and **11c** afforded (2:1 ligand-to-metal) complexes upon reaction with $Zn(OAc)_2$. Hydroxamates are considered excellent chelators for metal ion transport through cell membranes [34], whereas both the hydroxamate [34] and the sulfonamide [35] functionalities are of high medicinal relevance and are present in many bioactive compounds.

Biological evaluation of the effect of compounds on the insulin/PI3K/PTEN/Akt pathway

Zinc complexes induce Akt activation

The zinc(II) ion and some of its complexes have been reported in the past to elicit activation of Akt in several cell types [23, 36–39]. The activation of Akt in these cases occurs via the PI3K route and can be monitored by detecting the level of phosphorylation of residue Thr-308

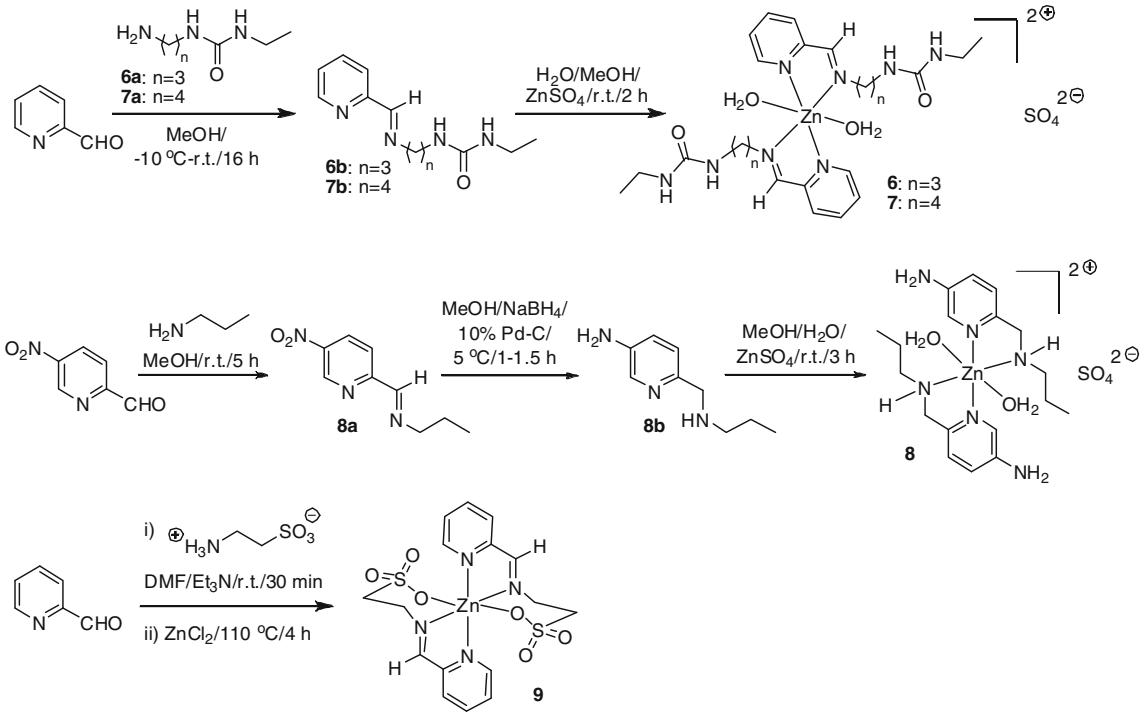

Scheme 3 Synthesis of pyridino zinc(II) complexes **6–9** (yields **6** 83%, **7** 51%, **8** 30%, **9** 20%)

Scheme 4 Synthesis of hydroxamic zinc(II) complexes **10** and **11** (yields **10** 92%, **11** 84%). *DCM* dichloromethane, *Tf_2O* trifluoromethane sulfonic anhydride

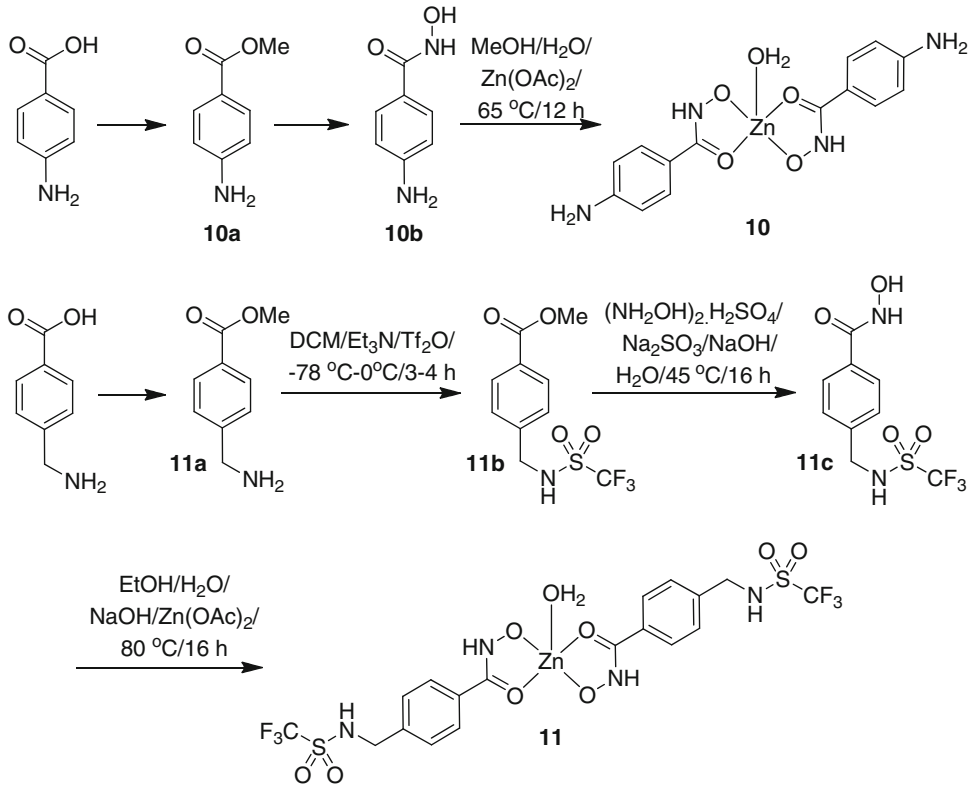

or residue Ser-473 of Akt. To examine whether the new zinc complexes prepared in this study induce Akt activation, NIH3T3 cells were treated with a 10 μM concentration of each compound, followed by light stimulation with 0.04 μM insulin. Western blots were run from the cell lysates and phospho-Akt was quantified using a phospho-Akt (Ser-473) antibody. Total Akt was also quantified as a loading control. Figure 3 summarizes these results.

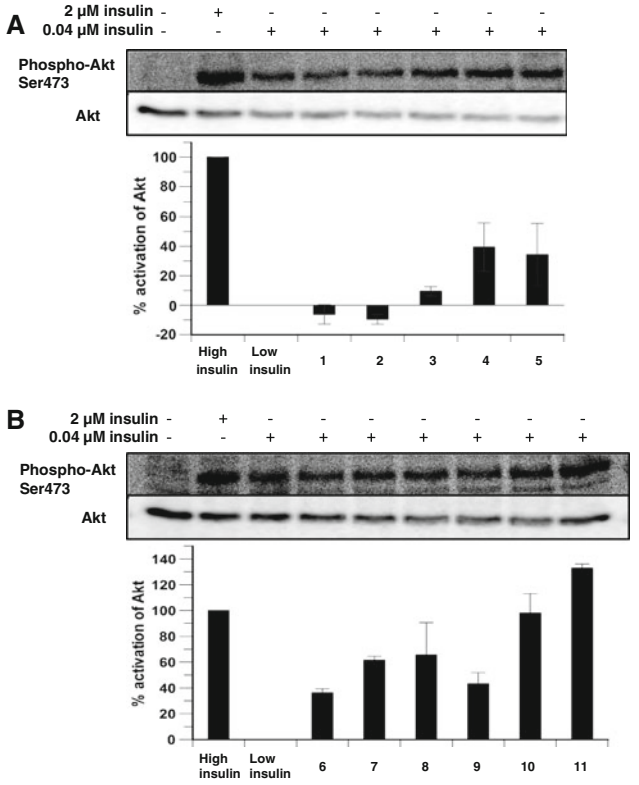

Fig. 3 **a** Compounds **1–5** and **b** compounds **6–11**. NIH3T3 cells were starved overnight, incubated with 10 μM compound (or vehicle) for 15 min, followed by insulin stimulation as indicated. Cells were collected and analyzed by western blotting using phospho-Akt (Ser-473) and Akt antibodies. The blots were quantified using ImageJ. The percentage of activation of Akt (Akt phosphorylation normalized for loading using the Akt blotting intensities) is shown. Low insulin stimulation (0.04 μM) was set to 0% and high insulin stimulation (2 μM) was set to 100%, respectively.The results (*bar chart*) are presented as the mean ± the standard deviation of three independent experiments

A positive control (stimulation with high insulin concentration, 2 μM) and a negative control (low insulin concentration equal to the concentration used to activate the insulin receptor, 0.04 μM) were included for comparison. All compounds, with the exception of **1–3**, whose effect is negligible, appear to activate Akt by elevating phospho-Akt levels to different extents. Although most of the compounds exhibit Akt activation to around 50% of that of the positive control, the two compounds derived from hydroxamic acid ligands (**10** and **11**) stand out, as they appear to perform equally effectively as or considerably better than the high insulin activation control, respectively.

Compound **11**, as the most promising Akt activator, was submitted to further investigation. First, we determined the cytotoxicity of this compound with the 3-(4,5-dimethylthiazol-2-yl)-2,5-diphenyltetrazolium bromide (MTT) assay on NIH3T3 cells [40]. MTT is reduced to formazan by living cells, and this reduction can be quantified using a spectrophotometer from the absorbance at 590 nm. As can be seen in Fig. 4, compound **11** shows cytotoxic effects on NIH3T3 cells at concentrations equal to or higher than 100 μM. At the 10 μM concentration, which was used in the initial screen of all 11 compounds (Fig. 3), compound **11** has no cytotoxic effect on the cells.

To determine the minimum concentration of compound **11** required to induce Akt activation, NIH3T3 cells were treated with various concentrations of the complex. As can be seen in Fig. 5a, Akt activation commenced at a 500 nM concentration of compound **11**. Moreover, when probing the compound-treated cell lysates for glycogen synthase kinase 3β (GSK-3β) phosphorylation at Ser-9, we found that **11** was also able to stimulate GSK-3β phosphorylation with similar potency (Fig. 5a). GSK-3β, a key enzyme in

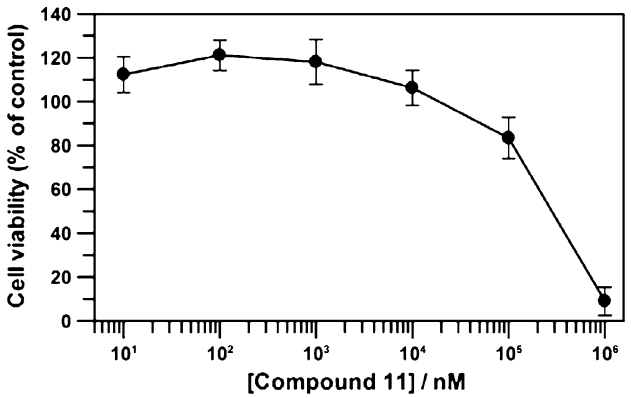

Fig. 4 Cytotoxicity of compound **11**. NIH3T3 cells were treated with up to 1 mM compound **11**. The results are presented as the mean ± the standard deviation ($n = 4$)

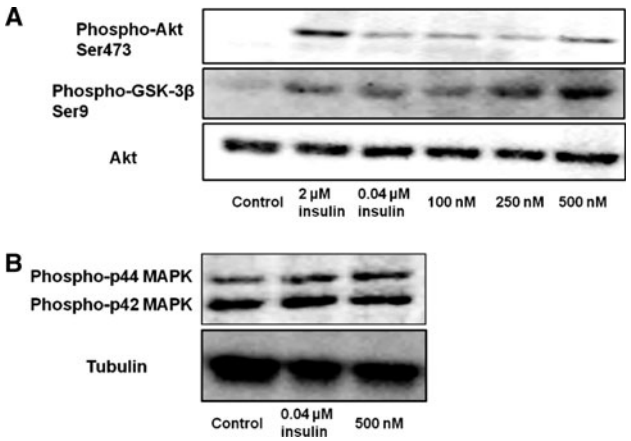

Fig. 5 **a** Activation of Akt and the downstream element GSK-3β (Ser-9) with compound **11** at various concentrations. Starved cells were incubated with 100, 250, and 500 nM compound **11** for 15 min, followed by stimulation of insulin at a concentration of 0.04 μM. **b** Compound **11** does not increase phosphorylation levels of p44 and p42 mitogen-activated protein kinase (*MAPK*). Same cell lysates (from **a**) were probed with a phospho-p44/phospho-p42 MAPK (Thr-202/Tyr-204) antibody

the regulation of glucose metabolism, is phosphorylated at Ser-9 by Akt, suggesting that the activation of Akt induced by the zinc complexes is propagated downstream of Akt to enhance glycogen synthesis. For comparison, the effect of compound **11** on the mitogen-activated protein kinase (MAPK) pathway was investigated by probing cellular extracts for phosphorylation of p42 and p44 MAPKs. As shown in Fig. 5b, compound **11** fails to activate p44 and p42 MAPKs at a concentration of 500 nM, implying that compound **11** might be a useful chemical tool to probe glucose metabolism and the signaling controlling it.

Zinc-complex-induced Akt activation is PI3K-dependent

To investigate whether the observed Akt phosphorylation is PI3K-mediated, we studied the effects of compound **11** on Akt phosphorylation levels in the presence of LY-294002, a known PI3K inhibitor [41]. If the observed Akt activation is PI3K-dependent, the presence of LY-294002 would be expected to abolish the activation induced by the zinc compound. Indeed, use of LY-294002 abrogated the phosphorylation of Akt induced by compound **11** as shown in Fig. 6. To further confirm the hypothesis that the zinc-complex-mediated activation occurs via PI3K, we examined whether any of the prepared complexes can induce Akt activation without any insulin stimulation. Notably, when there is complete deprivation of insulin, the compounds are unable to induce Akt phosphorylation (Fig. 7), which suggests they do not act directly at the insulin receptor level, but rather between the receptor and PI3K. Taking these observations together, we suggest that the zinc compounds induce Akt activation in a PI3K-dependent fashion.

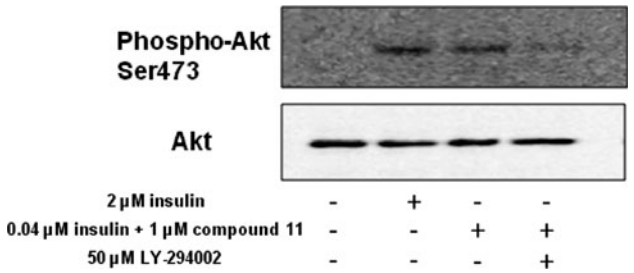

Fig. 6 Effects of compound **11** on Akt phosphorylation with and without the PI3K inhibitor LY-294002

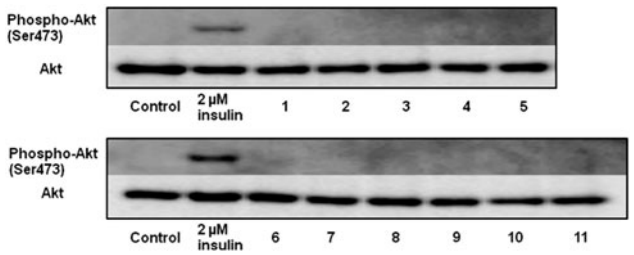

Fig. 7 Phospho-Akt (Ser-473) blots after cells were treated either with the zinc complexes without any insulin stimulation or with insulin (2 μM). The loading control was performed using the detection of total Akt

Zinc-complex-induced Akt activation is not via inhibition of PTPs or PTEN

The PI3K/Akt cascade is modulated by phosphatases of the PTP family and PTEN. PTPs oppose the signaling mediated by receptor tyrosine kinases by removing tyrosine phosphorylation, whereas PTEN directly antagonizes PI3K by dephosphorylating phosphatidylinositol 3,4,5-trisphosphate, the product of PI3K activity. As both PTPs and PTEN are upstream of Akt, their phosphatase activity can influence the level of Akt activation. Indeed, it has been found that inhibition of PTPs and PTEN will increase the cellular activity of Akt [42, 43].

Zinc(II) has been reported to have the ability to inhibit phosphatases such as λ-phosphoprotein phosphatase [44], PTP 1B [45], as well as PTEN [24]. To investigate whether the observed Akt activation was due to inhibition of PTEN and PTPs, the two most promising Akt-activating compounds (hydroxamic subset; **10** and **11**) were evaluated as PTEN and PTP-β inhibitors in vitro. As shown in Fig. 8, the inhibition of PTP-β and PTEN by compounds **10** and **11** revealed a significantly higher potency toward PTP-β, but failed to demonstrate the nanomolar potency achieved for Akt phosphorylation *in cellulo*. A similar picture was observed for other representative members of the series (results not shown).

Conclusion

In summary, a series of 11 novel zinc(II) complexes incorporating medicinally relevant functionalities were prepared based on phenolic, picolinic, pyridino, and hydroxamic ligands. Screening of the compounds for their potential to upregulate Akt phosphorylation *in cellulo* revealed a sulfonamide-containing hydroxamic complex as a potent activator of Akt at submicromolar concentrations. This lead structure can be potentially used as a chemical tool in diabetes research, owing to the fact that apart from activating Akt signaling, its effect is propagated downstream of Akt toward GSK-3β, an important regulator of glycogen synthesis/glucose metabolism. Our findings suggest that the observed effects on Akt phosphorylation by the hydroxamic zinc complexes, although PI3K-mediated, are not due to the inhibition of the tumor-suppressor phosphatase PTEN or PTPs. This signifies a departure from other zinc and vanadium complexes that have been shown to cause Akt activation by inhibiting these phosphatases.

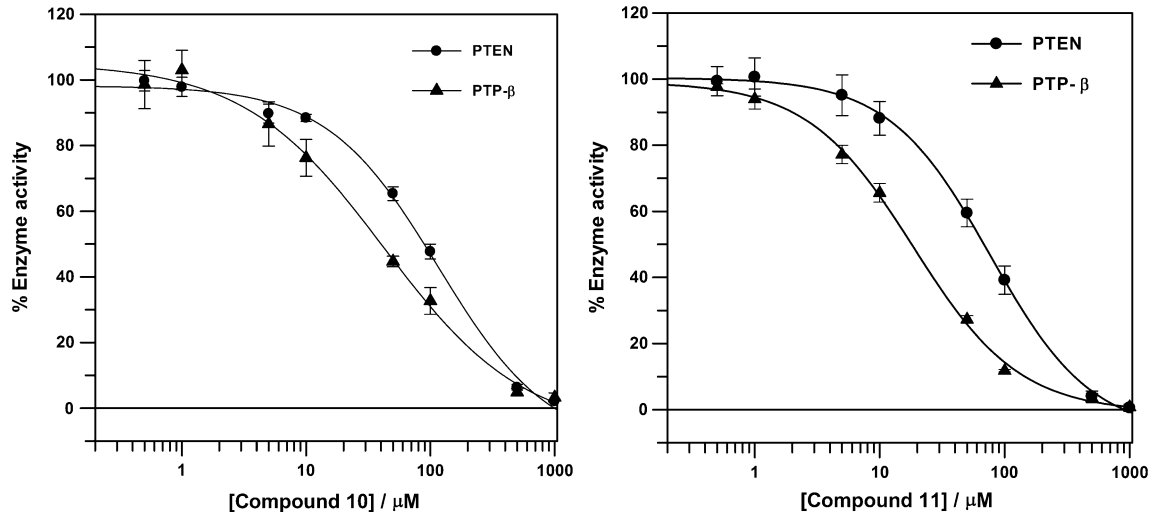

Fig. 8 Inhibition of PTEN and protein tyrosine phosphatase β (*PTP-β*) with zinc(II) complexes **10** and **11** using 3-*O*-methylfluorescein phosphate (OMFP) and *p*-nitrophenyl phosphate (p-NPP) as substrates. Recombinant PTEN and PTP-β were preincubated with either compound **10** or compound **11** at various concentrations at room temperature for 10 min. Reactions were initialized by adding 200 μM OMFP for PTEN and 1 mM p-NPP for PTP-β. The IC_{50} in the presence of compound **10** was calculated to be 116 ± 25 μM for PTEN and 42 ± 7 μM for PTP-β. The IC_{50} of compound **11** was determined to be 77 ± 5 μM for PTEN and 19 ± 1 μM for PTP-β. The results are presented as the mean ± the standard deviation of three independent experiments

Future research will be directed toward elucidating the exact mechanism of action of hydroxamic zinc complexes on Akt activation, as well as the development of improved Akt activators based on evolution of this novel template.

Materials and methods

General procedures

The purity of the organic chemicals was verified by ^{1}H-NMR spectroscopy. ^{1}H-NMR and ^{13}C-NMR spectra were recorded with a Bruker Avance 400 MHz Ultrashield NMR spectrometer. Infrared spectra were recorded with a Perkin Elmer Fourier transform infrared spectrometer. Electrospray ionization (ESI) mass spectra were recorded with a Bruker Daltronics Esquire 3000 spectrometer. Elemental analyses were performed by either London Metropolitan University or the University of Cambridge. The following compounds were prepared following literature procedures: **1a** [25], **5a** [30], **10a** [31], **10b** [33], and **11a** [32].

Synthesis

*Synthesis of **1***

Intermediate **1a** (0.107 g, 0.35 mmol, 1 equiv) was suspended in 45 mL of methanol. Ethanolamine (42 μL, 0.70 mmol, 2 equiv) was added and the mixture was stirred at room temperature overnight. The resulting solution was then cooled to 0 °C and 2 mL of a methanolic solution of $NaBH_4$ (0.026 g, 0.70 mmol, 2 equiv) was added dropwise. The mixture was stirred initially at 0 °C for 1 h, then allowed to warm up to room temperature. It was then filtered and the yellow precipitate collected was washed with methanol and dried to afford 43% of reductive amination product (0.053 g, 0.15 mmol). This compound was then dissolved in 10 mL of water to afford a clear solution. Aqueous 0.6 M HCl (0.25 mL, 0.15 mmol, 1 equiv) was added to the solution and the mixture was stirred briefly at room temperature, before the solvent was evaporated to dryness. The solid residue obtained was washed with diethyl ether to afford complex **1** in nearly quantitative yield (0.058 g, 0.15 mmol). ^{1}H-NMR (D_2O, 4.79 ppm) δ (ppm): 3.07 (t, 2H, $J = 5.4$ Hz), 3.75 (t, 2H, $J = 5.4$ Hz), 4.06 (s, 2H), 4.08 (s, 2H), 6.69 (bd, 1H, $J = 8.6$ Hz), 7.24 (m, 2H), 8.26 (s, 1H). ^{13}C-NMR (D_2O) δ (ppm): 48.1, 50.4, 56.7, 56.8, 119.5, 122.4, 126.0, 135.2, 137.6, 149.9, 168.9. Elemental analysis: calculated for $C_{12}H_{19}ClN_2O_6Zn$: C 37.13, H 4.93, N 7.22; found: C 36.57, H 4.12, N 6.96.

*Synthesis of **2***

Racemic homocysteic acid (0.150 g, 0.82 mmol, 1 equiv) was added to 5 mL of water and the resulting mixture was heated at 70 °C. A solution of 3-formyl-4-hydroxybenzenesulfonic acid disodium salt (0.201 g, 0.82 mmol, 1 equiv) in 5 mL of water was then added and the mixture was stirred at 70 °C for 90 min. A solution of $Zn(OAc)_2{\cdot}2H_2O$ (0.223 g, 1.02 mmol, 1.24 equiv) in 10 mL of water was finally added. During this last addition, the pH of the solution was adjusted to about 7 with aqueous NaOH

(0.5 M). The solution was stirred at 70 °C for a further 2 h. The solvent was then evaporated to dryness and a yellow-orange residue was obtained. Successive recrystallizations in water/methanol yielded compound **2** as a white solid in 54% yield (0.217 g, 0.44 mmol). ^{1}H-NMR (D_2O, 4.79 ppm) δ (ppm): 2.25 (m, 2H), 2.86 (m, 2H), 4.03 (t, 1H, $J = 6.2$ Hz), 6.72 (d, 1H, $J_1 = 9.0$ Hz), 7.57 (dd, 1H, $J_1 = 9.0$ Hz, $J_2 = 2.5$ Hz), 7.66 (d, 1H, $J_2 = 2.5$ Hz), 8.38 (s, 1H). ^{13}C-NMR (D_2O) δ (ppm): 29.9, 46.8, 66.3, 118.4, 122.2, 128.5, 130.9, 133.9, 169.7, 171.1, 179.1. Elemental analysis: calculated for $C_{11}H_{13}NNa_2O_{11}S_2Zn\cdot 2H_2O$: C 24.16, H 3.16, N 2.56; found: C 24.42, H 3.33, N 2.54.

*Synthesis of **3a***

3-Formyl-4-hydroxybenzenesulfonic acid disodium salt (0.300 g, 1.22 mmol, 1 equiv) was dissolved in 40 mL of methanol, and propylamine (0.121 mL, 1.47 mmol, 1.2 equiv) was added. The solution was stirred at room temperature for 3 h, at which point an aliquot was obtained to verify by NMR that the imine intermediate had formed. The solution was then cooled in an ice-bath and $NaBH_4$ (0.185 g, 4.88 mmol, 4 equiv) was added. The mixture was stirred at 0 °C for 1 h and at room temperature overnight. A few drops of water were added and then the solvent was evaporated to dryness. The residue was redissolved in methanol and insoluble impurities were removed by filtration. The filtrate was concentrated under a vacuum and diethyl ether was added to precipitate the product. Compound **3a** was obtained as a pink solid in 72% yield (0.255 g, 0.88 mmol). ^{1}H-NMR (D_2O, 4.79 ppm) δ (ppm): 0.85 (t, 3H, $J = 7.4$ Hz), 1.58 (bs, 2H), 2.88 (t, 2H, $J = 7.4$ Hz), 4.02 (s, 2H), 6.55 (d, 1H, $J = 8.6$ Hz), 7.45 (m, 2H). This ligand was used for the synthesis of **3** without any further purification.

*Synthesis of **3***

To a solution of **3a** (0.100 g, 0.35 mmol, 1 equiv) in 10 mL of methanol was added a solution of $Zn(OAc)_2\cdot 2H_2O$ (0.038 g, 0.175 mmol, 0.5 equiv) in 5 mL of methanol and the resulting mixture was stirred at 50 °C overnight. The solvent was evaporated to dryness and complex **3** was obtained as a yellow residue. It was further purified by recrystallization in methanol/diethyl ether to afford 70% (0.081 g, 0.12 mmol) of **3**. ^{1}H-NMR (D_2O, 4.79 ppm) δ (ppm): 0.86 (t, 6H, $J = 7.1$ Hz), 1.59 (bs, 4H), 2.90 (bt, 4H, $J = 6.7$ Hz), 4.06 (s, 4H), 6.63 (d, 2H, $J = 9.2$ Hz), 7.59 (m, 4H). Also present was 1 equiv of NaOAc impurity: 1.82 (s, 3H). Elemental analysis: calculated for $C_{20}H_{26}N_2Na_2O_8S_2Zn\cdot NaOAc$: C 38.86, H 4.30, N 4.12; found: C 38.77, H 4.41, N 3.98.

*Synthesis of **4***

A solution of ethylenediamine (0.027 mL, 0.41 mmol, 0.5 equiv) in 2 mL of methanol was added to a solution of 3-formyl-4-hydroxybenzenesulfonic acid disodium salt (0.202 g, 0.82 mmol, 1 equiv) in 40 mL of methanol and the reaction mixture was stirred at room temperature for 1 h. $Zn(OAc)_2\cdot 2H_2O$ (0.090 g, 0.41 mmol, 0.5 equiv) was then added and the mixture was heated at 50 °C overnight. It was subsequently filtered, and the white residue collected was washed with cold methanol and dried under a vacuum to afford **4** in 95% yield (0.216 g, 0.39 mmol). ^{1}H-NMR (D_2O, 4.79 ppm) δ (ppm): 3.79 (s, 4H), 6.80 (d, 2H, $J_1 = 8.9$ Hz), 7.55 (dd, 2H, $J_1 = 8.9$ Hz, $J_2 = 2.5$ Hz), 7.64 (d, 2H, $J_2 = 2.5$ Hz), 8.43 (s, 2H). ^{13}C-NMR (D_2O) δ (ppm): 55.8, 119.2, 122.6, 128.3, 130.0, 133.1, 168.1, 170.8. Elemental analysis: calculated for $C_{16}H_{14}N_2Na_2O_9S_2Zn\cdot 0.5H_2O$: C 34.15, H 2.69, N 4.98; found: C 34.11, H 2.72, N 4.89.

*Synthesis of **5***

A solution of $ZnSO_4\cdot 7H_2O$ (0.050 g, 0.175 mmol, 0.5 equiv) in 1.5 mL of water was added to a solution of **5a** (0.080 g, 0.35 mmol, 1 equiv) in 3 mL of ethanol/dimethylformamide (1:1). Aqueous NaOH (0.5 M, 0.7 mL, 0.35 mmol, 1 equiv) was added and the mixture was stirred at room temperature for 3 h. The resulting precipitate was then filtered off, washed with water, and dried under a vacuum to furnish 34% of complex **5** (0.033 g, 0.06 mmol). ^{1}H-NMR [dimethyl sulfoxide (DMSO)-d_6, 2.50 ppm] δ (ppm): 4.34 (d, 4H, $J = 5.2$ Hz), 7.12 (d, 2H, $J = 7.2$ Hz), 7.24 (m, 2H), 7.32 (m, 8H), 7.45 (bs, 2H), 7.85 (d, 2H, $J = 8.8$ Hz), 7.94 (bs, 2H). Elemental analysis: calculated for $C_{26}H_{26}N_4O_6Zn$: C 56.17, H 4.71, N 10.08; found: C 56.18, H 4.60, N 10.14.

*Synthesis of **6a***

Ethyl isocyanate (0.29 mL, 3.66 mmol, 1 equiv) was slowly added to a cooled solution (−10 °C) of 1,3-diaminopropane (0.305 mL, 3.66 mmol, 1 equiv) in 35 mL of CH_2Cl_2. The mixture was then stirred overnight at room temperature, resulting in precipitation of the desired urea product (**6a**). This solid was collected by filtration. Additionally, the filtrate was dried under a vacuum to yield an oily residue, which upon treatment with diethyl ether afforded more of the product. The combined product was washed with diethyl ether and dried. Overall, 63% of **6a** was obtained (0.335 g, 2.31 mmol). ^{1}H-NMR (DMSO-d_6, 2.50 ppm) δ (ppm): 0.95 (t, 3H, $J = 7.0$ Hz), 1.40 (m, 2H), 2.50 (m, 2H), 3.05 (m, 4H), 5.80 (bs, 2H). Liquid chromatography–mass spectrometry (LC–MS) (ESI^+):

calculated for $C_6H_{15}N_3O$ (M+H) 146.13, found 146.13. This compound was used in the next step without any further purification.

*Synthesis of **6b***

Pyridine-2-carboxaldehyde (0.10 mL, 1.0 mmol, 1 equiv) was slowly added (over 10 min) to a cold solution (−10 °C) of **6a** (0.145 g, 1.0 mmol, 1 equiv) in 2 mL of methanol, and the mixture was stirred overnight at room temperature. The solvent was then removed under a vacuum to yield a white residue, which was washed several times with diethyl ether and dried to furnish 93% of **6b** (0.217 g, 0.93 mmol). ^{1}H-NMR (DMSO-d_6, 2.50 ppm) δ (ppm): 0.97 (t, 3H, $J = 7.2$ Hz), 1.73 (m, 2H), 2.98 (m, 2H), 3.05 (apparent q, 2H, $J = 6.4$ Hz), 3.62 (t, 2H, $J = 6.8$ Hz), 5.76 (t, 1H, $J = 5.6$ Hz), 5.86 (t, 1H, $J = 5.6$ Hz), 7.45 (m, 1H), 7.86 (td, 1H, $J_1 = 7.6$ Hz, $J_2 = 1.2$ Hz), 8.34 (s, 1H), 8.63 (d, 1H, $J = 4.8$ Hz), 8.94 (d, 1H, $J_1 = 7.6$ Hz). ^{13}C-NMR (DMSO-d_6, 39.52 ppm) δ (ppm): 16.2, 31.6, 34.5, 37.7, 58.4, 120.9, 125.5, 137.3, 149.8, 154.6, 158.5, 162.4. Elemental analysis: calculated for $C_{12}H_{18}N_4O$: C 61.52, H 7.74, N 23.91; found: C 61.52, H 7.64, N 23.84.

*Synthesis of **6***

A solution of $ZnSO_4{\cdot}7H_2O$ (0.100 g, 0.35 mmol, 0.5 equiv) in 2 mL of water was added to a solution of **6b** (0.163 g, 0.70 mmol, 1 equiv) in 2 mL of methanol, and the resulting mixture was stirred at room temperature for 2 h. The solvent was then removed under a vacuum, yielding complex **6** as a pale-brown solid in 83% yield (0.193 g, 0.29 mmol). ^{1}H-NMR (DMSO-d_6, 2.50 ppm) δ (ppm): 0.88 (t, 6H, $J = 7.2$ Hz), 1.74 (m, 4H), 2.86 (m, 4H), 3.01 (apparent quartet, 4H, $J = 5.6$ Hz), 3.65 (bs, 4H), 5.85 (bs, 2H), 6.17 (bs, 2H), 7.66 (bs, 2H), 7.94 (d, 2H, $J = 7.6$ Hz), 8.08 (bs, 2H), 8.52 (s, 2H), 8.78 (bs, 2H). Elemental analysis: calculated for $C_{24}H_{40}N_8O_8SZn{\cdot}H_2O$: C 42.14, H 6.19, N 16.38; found: C 42.33, H 5.69, N 16.33.

*Synthesis of **7a***

This compound was prepared in 28% yield, following a method analogous to that used for the synthesis of **6a**. ^{1}H-NMR (DMSO-d_6, 2.50 ppm) δ (ppm): 0.95 (t, 3H, $J = 7.1$ Hz), 1.40 (m, 4H), 2.50 (bt, 2H, overlapping with DMSO peak), 3.00 (m, 4H), 5.71 (bt, 1H), 5.80 (bt, 1H). LC–MS (ESI$^+$): calculated for $C_7H_{17}N_3O$ (M+H) 160.15, found 160.15. This compound was used in the next step without any further purification.

*Synthesis of **7b***

This compound was prepared in 99% yield, following a method analogous to that used for the synthesis of **6b**. ^{1}H-NMR (DMSO-d_6, 2.50 ppm) δ (ppm): 0.96 (t, 3H, $J = 7.2$ Hz), 1.40 (m, 2H), 1.61 (m, 2H), 2.99 (m, 4H), 3.62 (t, 2H, $J = 7.2$ Hz), 5.71 (t, 1H, $J = 5.6$ Hz), 5.80 (t, 1H, $J = 5.2$ Hz), 7.45 (m, 1H), 7.86 (td, 1H, $J_1 = 7.6$ Hz, $J_2 = 1.2$ Hz), 7.93 (d, 1H, $J_1 = 7.6$ Hz), 8.33 (s, 1H), 8.63 (d, 1H, $J = 4.8$ Hz). ^{13}C-NMR (DMSO-d_6, 39.52 ppm) δ (ppm): 16.2, 28.2, 28.4, 34.5, 60.6, 120.8, 125.5, 137.3, 149.8, 154.6, 158.5, 162.1. Elemental analysis: calculated for $C_{13}H_{20}N_4O$: C 62.88, H 8.12, N 22.56; found: C 62.96, H 8.09, N 22.48.

*Synthesis of **7***

This compound was prepared in 51% yield, following a method analogous to that used for the synthesis of **6**. ^{1}H-NMR (DMSO-d_6, 2.50 ppm) δ (ppm): 0.93 (t, 6H, $J = 7.2$ Hz), 1.31 (m, 4H), 1.61 (m, 4H), 2.95 (m, 8H), 3.60 (bs, 4H), 5.93 (bs, 2H), 6.02 (bs, 2H), 7.67 (bs, 2H), 7.97 (d, 2H, $J = 7.6$ Hz), 8.10 (bs, 2H), 8.53 (s, 2H), 8.82 (bs, 2H). Elemental analysis: calculated for $C_{26}H_{44}N_8O_8SZn{\cdot}2.5H_2O$: C 42.25, H 6.68, N 15.16; found: C 42.13, H 5.89, N 15.16.

*Synthesis of **8a***

A solution of 5-nitropyridine-2-carboxaldehyde (0.386 g, 2.54 mmol, 1 equiv) in 20 mL of dry methanol was added dropwise to a solution of propylamine (0.24 mL, 2.92 mmol, 1.15 equiv) in 8 mL of methanol. The mixture was stirred for 5 h at room temperature and the solvent was then removed under a vacuum, to afford **8a** quantitatively as a dark oil (0.49 g, 2.54 mmol). ^{1}H-NMR ($CDCl_3$, 7.26 ppm) δ (ppm): 1.00 (t, 3H, $J = 7.4$ Hz), 1.79 (apparent sextet, 2H, $J = 7.2$ Hz), 3.73 (td, 2H, $J_1 = 6.9$ Hz, $J_2 = 1.3$ Hz), 8.23 (d, 1H, $J_3 = 8.7$ Hz), 8.47 (bs, 1H), 8.53 (dd, 1H, $J_3 = 8.7$ Hz, $J_4 = 2.4$ Hz), 9.47 (d, 1H, $J_4 = 2.4$ Hz). ^{13}C-NMR ($CDCl_3$, 77.00 ppm) δ (ppm): 11.9, 23.8, 63.5, 121.21, 131.6, 144.4, 144.9, 159.2, 159.9. This compound was used for the next step without any further purification.

*Synthesis of **8b***

A solution of **8a** (0.293 g, 1.52 mmol, 1 equiv) in 25 mL of dry methanol was mixed with 0.09 g of 10% Pd–C and cooled to 5 °C. $NaBH_4$ (0.23 g, 6.1 mmol, 4 equiv) was added portionwise to the mixture over 30 min. The resulting solution was stirred at the same temperature for 1 h, then allowed to warm up to room temperature. It was

subsequently filtered through Celite and the solvent was evaporated to dryness. The remaining residue was resuspended in ethyl acetate and the organic phase was washed with water. The aqueous phase was back-extracted with $CHCl_3$. All organic fractions were dried over $MgSO_4$ and the solvent was evaporated to dryness to afford **8b** as a yellow oil in 55% yield (0.139 g, 0.84 mmol). ^{1}H-NMR ($CDCl_3$, 7.26 ppm) δ (ppm): 0.93 (m, 3H), 1.54 (m, 2H), 2.61 (m, 2H), 3.66 (bs, 2H), 3.79 (s, 2H), 6.96 (dd, 1H, $J_1 = 8.2$ Hz, $J_2 = 2.8$ Hz), 7.09 (d, 1H, $J_1 = 8.2$ Hz), 8.06 (d, 1H, $J_2 = 2.8$ Hz). ^{1}H-NMR (DMSO-d_6, 2.50 ppm) δ (ppm): 0.85 (m, 3H), 1.41 (m, 2H), 2.46 (m, 2H), 3.60 (s, 2H), 5.13 (bs, 2H), 6.88 (dd, 1H, $J_1' = 8.3$ Hz, $J_2' = 2.7$ Hz), 7.03 (d, 1H, $J_1' = 8.3$ Hz), 7.85 (d, 1H, $J_2' = 2.7$ Hz). ^{13}C-NMR ($CDCl_3$, 77.00 ppm) δ (ppm): 11.8, 23.2, 51.5, 54.7, 122.3, 122.6, 136.9, 141.0, 149.9. ^{13}C-NMR (DMSO-d_6, 39.52 ppm) δ (ppm): 12.3, 22.9, 51.1, 54.4, 121.0, 122.4, 135.8, 143.7, 147.3. This compound was used for the next step without any further purification.

*Synthesis of **8***

A solution of $ZnSO_4 \cdot 7H_2O$ (0.121 g, 0.42 mmol, 0.5 equiv) in 10 mL of methanol was added to a solution of **8b** (0.139 g, 0.84 mmol, 1 equiv) in 10 mL of methanol, and the resulting mixture was stirred at room temperature for 3 h. The solvent was then evaporated to dryness and the residue was washed with CH_2Cl_2 and ethyl ether. Recrystallization in methanol/diethyl ether afforded complex **8** as a yellow solid in 30% yield (0.066 g, 0.125 mmol). ^{1}H-NMR (DMSO-d_6, 2.50 ppm) δ (ppm): 0.81 (t, 6H, $J = 7.3$ Hz), 1.50 (m, 4H), 2.62 (bs, 4H), 3.80 (bs, 4H), 5.58 (bs, 2H), 5.71 (bs, 4H), 7.18 (bs, 4H), 8.03 (bs, 2H). ^{13}C-NMR (DMSO-d_6, 39.52 ppm) δ (ppm): 11.8, 20.9, 50.3, 50.4, 123.3, 123.7, 134.7, 142.4, 145.6. LC–MS (ESI^+): calculated for $C_{18}H_{28}N_6Zn$ (M+H) 393.18, found 393.18. IR (cm^{-1}): 1,118 (SO_4^{2-}), 1,506 (m), 1,581 (m), 1,630 (m), 1,735 (br), 2,875 (br), 2,964 (br), 3,229, 3,349. Elemental analysis: calculated for $C_{18}H_{34}N_6O_6SZn \cdot 2H_2O$: C 38.33, H 6.79, N 14.90; found: C 38.58, H 6.15, N 14.27.

*Synthesis of **9***

Pyridine-2-carboxaldehyde (0.19 mL, 2 mmol, 1 equiv) was dissolved in 50 mL of dimethylformamide in a round-bottom flask. Taurine (0.25 g, 2 mmol, 1 equiv) was added to this solution, followed by anhydrous triethylamine (0.28 ml, 2 mmol, 1 equiv). After the mixture had been stirred at room temperature to solubilize all components, $ZnCl_2$ was added (0.14 g, 1 mmol, 0.5 equiv) and the reaction mixture was heated at 110 °C for 4 h. The resulting precipitate was filtered and washed to afford **9** as a pink powder in 20% yield (0.10 g, 0.2 mmol). ^{1}H-NMR (DMSO-d_6, 2.50 ppm) δ (ppm): 3.03 (bs, 4H), 4.24 (bs, 4H), 7.67 (t, 2H, $J = 6.4$ Hz), 8.03 (d, 2H, $J = 8.0$ Hz), 8.17 (bs, 2H), 8.36 (bs, 2H), 8.88 (bs, 2H). ^{13}C-NMR (DMSO-d_6, 39.52 ppm) δ (ppm): 49.86, 54.46, 128.94, 141.11, 148.63, 163.60. IR (cm^{-1}): 738, 1,228, 1,530, 1,594, 2,943, 3,235, 3,331. Elemental analysis: calculated for $C_{16}H_{18}N_4O_6S_2Zn$: C 39.07, H 3.69, N 11.39; found: C 39.13, H 3.73, N 11.45.

*Synthesis of **10***

4-Amino-*N*-hydroxybenzamide (**10b**) (0.20 g, 1.32 mmol, 1 equiv) was transferred to a round-bottom flask and dissolved in methanol (13.2 mL). $Zn(OAc)_2 \cdot 2H_2O$ (0.145 g, 0.66 mmol, 0.5 equiv) was added, and the reaction mixture was refluxed at 65 °C for 12 h, during which a white precipitate formed. After the mixture had cooled to room temperature, it was filtered and the solid filtered off was washed several times with chilled water and dried under a vacuum. Overall, 92% (0.235 g, 0.61 mmol) of complex **10** was obtained. ^{1}H-NMR (DMSO-d_6, 2.50 ppm) δ (ppm): 5.50 (s, 4H), 6.53 (d, 4H, $J = 8.6$ Hz), 7.48 (d, 4H, $J = 8.6$ Hz), 11.50 (s, 2H). ^{1}H-NMR (D_2O, 4.79 ppm, with 1% formic acid-d_2) δ (ppm): 7.26 (d, 4H, $J = 8.0$ Hz), 7.71 (d, 4H, $J = 8.0$ Hz). LC–MS (ESI^+): calculated for $C_{14}H_{14}N_4O_4Zn$ (M+H) 367.04, found 367.04. IR (cm^{-1}): 1,504, 1,563, 1,598, 3,018, 3,170, 3,431. Elemental analysis: calculated for $C_{14}H_{16}N_4O_5Zn$: C 43.59, H 4.18, N 14.53; found: C 44.02, H 3.71, N 14.35.

*Synthesis of **11b***

Methyl 4-(aminomethyl)benzoate (**11a**) (1.65 g, 10 mmol, 1 equiv) was transferred to a round-bottom flask, which was then sealed and purged with nitrogen. Anhydrous CH_2Cl_2 (33 mL) was added and the mixture was cooled to −78 °C. Triethylamine (2.8 mL, 20 mmol, 2 equiv) was added, followed by dropwise addition of trifluoromethanesulfonic anhydride (1.7 mL, 10 mmol, 1 equiv) at −78 °C. The mixture was stirred for 3–4 h, with the temperature slowly rising to 0 °C. The reaction mixture was then diluted with CH_2Cl_2, and the resulting mixture was washed once with aqueous NH_4Cl (saturated), once with aqueous NaCl (saturated), and once with H_2O. The organic phase was dried over Na_2SO_4, then filtered and concentrated under a vacuum. The sample was applied to a silica column and eluted with hexane–ethyl acetate (first 2:1, then 1:1), to afford **11b** in 88% yield (2.61 g, 8.8 mmol) as a white solid. ^{1}H-NMR ($CDCl_3$, 7.26 ppm) δ (ppm): 3.92 (s, 3H), 4.51 (s, 2H), 5.43 (bs, 1H), 7.39 (d, 2H, $J = 8.3$ Hz), 8.01 (d, 2H, $J = 8.3$ Hz). ^{13}C-NMR ($CDCl_3$, 77.00 ppm) δ (ppm): 47.65, 52.37, 119.62 (CF_3 quartet),

127.61, 130.03, 130.19, 140.49, 166.89. LC–MS (ESI^+): calculated for $C_{10}H_{10}F_3NO_4S$ (M+H) 298.04, found 298.04. IR (cm^{-1}): 1,001, 1,018, 1,081, 1,119, 1,150, 1,181, 1,233, 1,289, 1,306, 1,386, 1,445, 1,615, 1,695, 3,229. Elemental analysis: calculated for $C_{10}H_{10}F_3NO_4S$: C 40.41, H 3.39, N 4.71; found C 40.51, H 3.27, N 4.64.

*Synthesis of **11c***

Hydroxylamine sulfate (0.82 g, 5 mmol, 1 equiv) was transferred to a round-bottom flask containing 5 g of ice. A solution of NaOH (1.0 g, 25 mmol, 5 equiv) in 5 mL of water was added to the flask and the mixture was stirred at room temperature for 5 min. A catalytic amount of Na_2SO_3 (0.095 g, 0.75 mmol, 0.15 equiv) and methyl 4-[(trifluoromethylsulfonamido)methyl]benzoate (**11b**) (1.49 g, 5 mmol, 1 equiv) were then added in solid form, and the mixture was heated at 45 °C for 16 h. After the mixture had cooled to room temperature, the pH was modified to about 5 by dropwise addition of 10% (w/w) aqueous H_2SO_4, and the solvent was removed under a vacuum. Cold methanol was added to the solid residue and the resulting suspension was vigorously stirred for 15 min and filtered. The hydroxamic acid, free of most inorganic impurities, was recovered by drying the methanolic filtrate. This sample was redissolved in 90:10 CH_2Cl_2–CH_3OH and applied to a silica column. Elution took place with the same solvent system (first 90:10, then 85:15) to afford 76% (1.13 g, 3.8 mmol) of hydroxamic acid **11c** as a white solid. ^{1}H-NMR (DMSO-d_6, 2.50 ppm) δ (ppm): 4.42 (s, 2H), 7.40 (d, 2H, $J = 8.1$ Hz), 7.75 (d, 2H, $J = 8.1$ Hz), 9.04 (s, 1H), 10.02 (s, 1H), 11.22 (s, 1H). ^{13}C-NMR (DMSO-d_6, 39.52 ppm) δ (ppm): 46.34, 119.69 (CF_3 quartet), 127.21, 127.38, 132.20, 140.22, 163.92. LC–MS (ESI^+): calculated for $C_9H_9F_3N_2O_4S$ (M+H) 299.03, found 299.03. IR (cm^{-1}): 1,511, 1,542, 1,577, 1,618, 3,388. Elemental analysis: calculated for $C_9H_9F_3N_2O_4S$: C 36.24, H 3.04, N 9.39; found C 36.25, H 3.02, N 9.11.

*Synthesis of **11***

N-Hydroxy-4-[(trifluoromethylsulfonamido)methyl]benzamide **11c** (0.63 g, 2.11 mmol, 1 equiv) was transferred to a round-bottom flask and dissolved in absolute ethanol (15 mL). A solution of NaOH (0.084 g, 2.11 mmol, 1 equiv) in 5 mL of water was added, and the mixture was stirred at room temperature for 5 min. Solid $Zn(OAc)_2{\cdot}2H_2O$ (0.23 g, 1.055 mmol, 0.5 equiv) was then added, and the reaction was refluxed at 80 °C for 16 h. The solvent was then removed under a vacuum and the solid residue was washed extensively with cold water and dried under a vacuum to afford complex **11** in 84% yield (0.60 g, 0.89 mmol), as a white solid**.** ^{1}H-NMR (DMSO-d_6, 2.50 ppm) δ (ppm): 4.27 (s, 4H), 7.35 (d, 4H, $J = 7.7$ Hz), 7.66 (d, 4H, $J = 7.7$ Hz), 11.82 (s, 2H). LC–MS (ESI^+): calculated for $C_{18}H_{16}F_6N_4O_8S_2Zn$ (M+H) 658.97, found 658.97. IR (cm^{-1}): 874, 918, 1,022, 1,056, 1,149, 1,190, 1,231, 1,372, 1,441, 1,503, 1,565, 1,606, 3,350 (br). Elemental analysis: calculated for $C_{18}H_{18}F_6N_4O_9S_2Zn{\cdot}H_2O$: C 31.07, H 2.90, N 8.05; found C 31.00, H 2.40, N 7.63.

Biological materials and methods

Cell culture and western blot analysis

NIH3T3 fibroblasts were purchased from ATCC. Cells were grown in Dulbecco's modified Eagle's medium (DMEM) (Sigma) supplemented with 10% (v/v) bovine calf serum (ATCC) in an atmosphere of 5% CO_2 at 37 °C. For testing the zinc complexes, cells were starved in DMEM (without serum) for 16 h at 37 °C. Subsequent to serum deprivation, cells were treated with zinc compounds for 15 min in DMEM at 37 °C. Following compound treatment, cells were stimulated with either 2 μM insulin or 0.04 μM insulin for 15 min. A control was included where cells were neither treated with zinc compounds nor stimulated with insulin. The cells were washed afterwards three times with ice-cold phosphate-buffered saline and then lysed in sodium dodecyl sulfate (SDS)–polyacrylamide gel electrophoresis buffer, containing 150 mM tris(hydroxymethyl)aminomethane (Tris–HCl), pH 6.8, 25% glycerol, 5% SDS, 5% β-mercaptoethanol, and 0.01% bromophenol blue. Cell lysates were separated on a 10% SDS–polyacrylamide gel and transferred onto a nitrocellulose membrane. Membranes were blocked with 5% skimmed milk in 50 mM Tris, 150 mM NaCl, 0.1% Tween 20, pH 7.4 (TBS/T) for 1 h at room temperature. Phospho-Akt (Ser-473) rabbit monoclonal antibody, mass-Akt rabbit polyclonal antibody, GSK-3β (Ser9) rabbit polyclonal antibody, and phospho-p44/p42 MAPK (Thr-202/Tyr-204) rabbit polyclonal antibody (Cell Signaling) were used as primary antibodies for immunoblotting analysis. Primary antibody incubation was performed in 5% bovine serum albumin in TBS/T for 16 h at 4 °C. Blots were washed for 15 min with TBS/T, then incubated with horseradish peroxidase conjugated secondary antibody (Bio-Rad) in blocking buffer for 1 h, and then probed with western blotting detection reagent (ECL, GE Healthcare).

PTEN expression and purification

PTEN was expressed as a glutathione *S*-transferase (GST) fusion protein and purified according to methods previously described [13]. Protein expression was induced in the *Escherichia coli* strain XL-1 blue for 24 h using 1 mM isopropyl β-D-1-thiogalactopyranoside at 23 °C. Cells were

harvested and stored at −20 °C. The harvested cells were resuspended in lysis buffer containing 50 mM Tris (pH 7.4), 1% Triton X-100, 10 mM benzamidine hydrochloride, 100 μg/mL soybean trypsin inhibitor, 1 mM 4-(2-aminoethyl)benzenesulfonyl fluoride hydrochloride, and 2 mM dithiothreitol (DTT). Lysis was performed by adding lysozyme to the cell suspension at a concentration of 2 mg/mL and sonication. Cell debris was removed by centrifugation at 18,000*g* for 1 h at 4 °C. The supernatant was loaded onto a glutathione Sepharose column, pre-equilibrated with 50 mM Tris (pH 7.4), 140 mM NaCl, and 2.7 mM KCl. After loading, the column was washed twice with 50 mM Tris (pH 7.4), 140 mM NaCl, 2.7 mM KCl, and 2 mM DTT. Another two washes were performed using the same buffer with 500 mM NaCl. The GST-tagged PTEN was eluted using 20 mM glutathione in 50 mM Tris (pH 7.4), 250 mM NaCl, 20% glycerol, and 2 mM DTT. Protein concentration was determined using the Bradford assay.

PTEN activity assay

PTEN activity in the presence of zinc compounds was assessed using the fluorescent substrate 3-*O*-methylfluorescein phosphate (OMFP) [46]. OMFP was dissolved in DMSO to a concentration of 20 mM and then further diluted with 1% DMSO to the concentrations tested. Assays were performed in 100 mM Tris (pH 7.4) containing 2 mM DTT at room temperature (20 °C). For inhibition studies, PTEN was preincubated with zinc compounds at room temperature for 10 min. Reactions were then initialized by adding OMFP to a final concentration of 200 μM. The hydrolysis of OMFP to 3-*O*-methylfluorescein was monitored by measuring the change of fluorescence units in a 96-well microtiter plate (excitation at 485 nm and emission at 525 nm) using a Varian fluorescence spectrophotometer.

Cytotoxicity assay

NIH3T3 cells were seeded into a 96-well plate at a concentration of 8,000 cells per well and incubated at 37 °C for 16 h. Cells were treated with compound **11** at concentrations between 10 nM and 1 mM for 2 h at 37 °C (total volume of 100 μL). After 2 h, 20 μL of a 5 mg/mL MTT solution was added to each well and the mixture was incubated for a further 4 h at 37 °C. The media were removed carefully, 150 μL of 4 mM HCl in isopropyl alcohol was added to each well, and the mixture was incubated at room temperature for 15 min on an orbital shaker. The formation of formazan by viable cells was measured using a spectrophotometer at 590 nm.

Acknowledgments This work was supported by the Leverhulme Trust, the Lowe Syndrome Trust, Imperial Innovations, and the Departament d'Educació i Universitats de la Generalitat de Catalunya. In addition, the UK's Engineering and Physical Sciences Research Council is thanked for a Leadership Fellowship to R.V.

References

1. Spring DR (2005) Chem Soc Rev 34:472
2. Lehar J, Stockwell BR, Giaever G, Nislow C (2008) Nat Chem Biol 4:674
3. Tarrant MK, Cole PA (2009) Annu Rev Biochem 78:797
4. Alonso A, Sasin J, Bottini N, Friedberg I, Friedberg I, Osterman A, Godzik A, Hunter T, Dixon J, Mustelin T (2004) Cell 117:699
5. Manning G, Whyte DB, Martinez R, Hunter T, Sudarsanam S (2002) Science 298:1912
6. Yaffe MB (2002) Nat Rev Mol Cell Biol 3:177
7. Yaffe MB, Elia AEH (2001) Curr Opin Cell Biol 13:131
8. Hunter T (2000) Cell 100:113
9. Gunn R, Hailes H (2008) J Chem Biol 1:49
10. Gonzalez E, McGraw T (2009) Cell Cycle 8:2502
11. Cicenas J (2008) Int J Biol Markers 23:1
12. Zhang W, Miao L (2007) Zhongfeng Yu Shenjing Jibing Zazhi 24:755
13. Rosivatz E, Matthews JG, McDonald NQ, Mulet X, Ho KK, Lossi N, Schmid AC, Mirabelli M, Pomeranz KM, Erneux C, Lam EWF, Vilar R, Woscholski R (2006) ACS Chem Biol 1:780
14. Tsuruzoe K, Araki E (2005) Diabetes Front 16:589
15. Asano T, Kamata H (2006) Idenshi Igaku Mook 6:255
16. Cuncic C, Detich N, Ethier D, Tracey AS, Gresser MJ, Ramachandran C (1999) J Biol Inorg Chem 4:354
17. Nxumalo F, Glover NR, Tracey AS (1998) J Biol Inorg Chem 3:534
18. Peters KG, Davis MG, Howard BW, Pokross M, Rastogi V, Diven C, Greis KD, Eby-Wilkens E, Maier M, Evdokimov A, Soper S, Genbauffe F (2003) J Inorg Biochem 96:321
19. Shechter Y, Goldwaser I, Mironchik M, Fridkin M, Gefel D (2003) Coord Chem Rev 237:3
20. Tracey AS (2000) J Inorg Biochem 80:11
21. Nishide M, Yoshikawa Y, Yoshikawa EU, Matsumoto K, Sakurai H, Kajiwara NM (2008) Chem Pharmacol Bull 56:1181
22. Sakurai H, Yoshikawa Y, Yasui H (2008) Chem Soc Rev 37:2383
23. Basuki W, Hiromura M, Sakurai H (2007) J Inorg Biochem 101:692
24. Nakayama A, Hiromura M, Adachi Y, Sakurai H (2008) J Biol Inorg Chem 13:675
25. Cai JH, Huang YH, Jiang YM (2006) Acta Crystallogr Sect E Struct Rep Online E62:m2432
26. Hall D, Moore FH (1966) J Chem Soc A 1822
27. Kojima Y, Yoshikawa Y, Ueda E, Kishimoto N, Tadokoro M, Sakurai H (2005) Bull Chem Soc Jpn 78:451
28. Nakai M, Sekiguchi F, Obata M, Ohtsuki C, Adachi Y, Sakurai H, Orvig C, Rehder D, Yano S (2005) J Inorg Biochem 99:1275
29. Yoshikawa Y, Ueda E, Kawabe K, Miyake H, Takino T, Sakurai H, Kojima Y (2002) J Biol Inorg Chem 7:68
30. Finch N, Campbell TR, Gemenden CW, Povalski HJ (1980) J Med Chem 23:1405
31. Hosangadi B, Dave RH (1996) Tetrahedron Lett 37:6375
32. Goodyer CLM, Chinje EC, Jaffar M, Stratford IJ, Threadgill MD (2003) Bioorg Med Chem 11:4189
33. Gaynor D, Starikova ZA, Haase W, Nolan KB (2001) J Chem Soc Dalton Trans 1578
34. Codd R (2008) Coord Chem Rev 252:1387

35. Bhat MA, Imran M, Khan SA, Siddiqui N (2005) Ind J Pharm Sci 67:151
36. Walter PL, Kampkoetter A, Eckers A, Barthel A, Schmoll D, Sies H, Klotz L-O (2006) Arch Biochem Biophys 454:107
37. Bao S, Knoell DL (2006) Am J Physiol 290:L433
38. Chanoit G, Lee S, Xi J, Zhu M, McIntosh RA, Mueller RA, Norfleet EA, Xu Z (2008) Am J Physiol 295:H1227
39. Wong VVT, Nissom PM, Sim S-L, Yeo JHM, Chuah S-H, Yap MGS (2006) Biotechnol Bioeng 93:553
40. Mosmann T (1983) J Immunol Methods 65:55
41. Vlahos CJ, Matter WF, Hui KY, Brown RF (1994) J Biol Chem 269:5241
42. Xie L, Lee S, Andersen J, Waters S, Shen K, Guo X (2003) Biochemistry 42:12792
43. Schmid A, Byrne R, Vilar R, Woscholski R (2004) FEBS Lett 566:35
44. Zhuo S, Dixon J (1997) Protein Eng 10:1445
45. Haase H, Maret W (2005) Biometals 18:333
46. Mak LH, Vilar R, Woscholski R (2010) J Chem Biol 3:157